JOURNAL OF PROPULSION AND POWER
Vol. 11, No. 6, November–December 1995

Experimental Studies into Hail Impact Characteristics

P. M. Render* and H. Pan†
Loughborough University of Technology, Loughborough, Leicestershire LE11 3TU, England, United Kingdom

A program of work to develop an understanding of hailstone impact characteristics is described and the progress to date is presented. Patternators and high-speed photography have been used to investigate impact characteristics on a flat plate and a spinner from a turbofan aeroengine. Results have shown that the approach angle of the hailstones, relative to the impact surface, has a significant effect on the distribution of ice following impact. Approach velocity of the hailstones, target temperature, and spinner rotation have no significant effect on the distribution. Studies into successive impacts on two adjacent surfaces have shown that the angle between the two surfaces is important in determining the distribution of ice.

Nomenclature

T = time after ice ball impact, ms
Y = distance between target and patternator, mm
θ_1 = approach angle to first plate in secondary impact studies, deg
θ_2 = angle of second plate, deg

Introduction

A RECENT Aerospace Industries Association (AIA) report[1] concerning the effects of inclement weather on aircraft operation has identified a small but significant number of uncommanded power loss events attributed to extreme rain/hail conditions. Many of these events occurred at low-engine power setting, e.g., during aircraft descent. As a result of the AIA work, recommendations to add to the existing certification requirements relating to rain and hail ingestion have been made. Engine compliance with current certification requirements relating to rain is usually demonstrated in ground-based tests where water is sprayed directly into the engine. The volume of water is representative of the extreme liquid water content that may be encountered by an aircraft operating in a rain storm. The extent to which these ground-based tests needs to be extended to cover aircraft operation in extreme rain/hail conditions is currently being considered by the certification authorities.

Water entering an engine in any form can, in the extreme, result in a power loss by several different mechanisms, including combustor flameout. More normal results include the stalling and surging of compressors, reduction of clearances between stationary and moving components, and the blockage of bleed valves. These last two items may result in the reduction of component efficiencies and corresponding problems with the engine control system. The performance and control implications of water entering an engine have been extensively studied by all of the major aeroengine manufacturers and at various research establishments (see, e.g., Murthy[2]).

Compared with rain, hail entering an engine intake differs in a number of respects. Firstly, hailstones do not break up as they enter into the engine intake. Secondly, hailstones are physically larger than water droplets with diameters ranging from 2 or 3 mm to 10 cm in extreme conditions. As the hailstones impact upon the spinner and blades of the fan, they are known to break up into fragments of ice. If the kinetic energy of the hailstones is sufficient there may also be a phase change at impact resulting in liquid water. Following the impact on the fan, the ice fragments, or water, may enter either the bypass duct or engine core. It is the ice entering the engine core that is of primary concern since water in the bypass duct has no discernable effect on engine control or performance. Surveys of meteorological data have shown that the highest concentration of hail water content in the atmosphere is most likely to occur at altitudes between 3600–4600 m[1]. The atmospheric surveys suggest that 10 g of hail per m^3 of air is typical for a severe hail storm.

The parameters that govern the impact characteristics of hailstones and the resulting trajectories of the ice fragments are unknown. All previous work concerning hailstone impact on aircraft and engines has been concerned with the structural integrity of the component struck by the hailstone. The trajectories and distribution of ice fragments resulting from the impact was of no concern and was not recorded. Given the lack of data in the public domain on hail ingestion, a wide-ranging study was initiated to do the following:

1) Devise techniques for studying the hail ingestion characteristics of turbofan engines.
2) Develop an understanding of the mechanisms involved in the breakup of hailstones following impact.
3) Determine the significance of seemingly important parameters (e.g., hailstone approach velocity).
4) Obtain experimental data suitable for developing mathematical models to describe hail impact characteristics on engine fans.
5) Develop computer software using the mathematical models, to predict the hail ingestion characteristics of turbofan engines.
6) Design and develop ground-based facilities to demonstrate safe engine operation in extreme hail conditions.

Experimental Program

The ultimate aim of the experimental program is to carry out hailstone impact tests on a rotating engine fan. The nature of the impacts is likely to be highly complicated, being dependent upon fan geometry, rotational speed, hailstone approach angle, etc. To isolate the effects of all the possible variables it was decided to carry out a series of experiments. The first of these experiments has been completed and included in the following:

1) Stationary flat plate: to gain an understanding of the basic impact characteristics, and to allow the importance of

Presented as Paper 93-2174 at the AIAA/SAE/ASME/ASEE 29th Joint Propulsion Conference, Monterey, CA, June 28–30, 1993; received Jan. 14, 1994; revision received Nov. 8, 1994; accepted for publication Feb. 18, 1995.

*Lecturer, Department of Aeronautical Engineering. Member AIAA.
†Research Assistant, Department of Aeronautical Engineering. Member AIAA.

hailstone parameters (approach speed, approach angle, etc.) to be assessed.

2) Stationary and rotating spinner tests: to assess the influence of spinner geometries on the flat plate results.

3) Secondary impact studies: to gain an understanding of impact characteristics when ice fragments from the first impact collide with a second surface. The results and conclusions are presented in the following sections.

Experimental Facilities and Technique

The hailstones (or ice balls) were made from flaked ice molded under pressure into 12.7-mm-diam spheres. This size is compatible with the draft requirements of the European Joint Aviation Authority, which is proposing ice ball diameters between 12–19 mm for hail ingestion tests. After molding, the ice balls were placed in a freezer at −14°C for 24 h to ensure that the balls were at a uniform temperature throughout their cross section. The flaked ice used for molding the ice balls was produced by a commercial ice maker connected to the water main. This water was not "pure," unlike the ice in naturally occurring hail. To assess the influence of the impurities in the tap water, some of the flat-plate tests were repeated using ice balls made from distilled water. There was no discernable difference in the results. During the experimental program a freezer capable of −40°C was procured and used in preference to the −14°C freezer, because the lower temperature is close to the atmospheric temperatures at which natural hailstones are formed. However, flat plate tests showed no measurable differences between ice balls stored in either freezer.

In this article the term ice ball will be used in preference to hailstone. The term hailstone will be restricted to the naturally occurring product of hailstorms.

The experimental arrangement is shown in Figs. 1 and 2 and is fully described by Render et al.[3] The compressed air-operated hail gun was used to fire ice balls at the target at speeds of up to 175 m/s. The speed of the ice ball was determined by the laser speed measurement device. This device consisted of three laser diode generated laser beams placed across the path of the ice ball. By measuring the time interval between the ice ball cutting any two beams it was possible to determine the ice ball's speed. In addition, by observing the outputs from the photoelectric cells it was possible to determine whether an ice ball broke before impact. Runs with broken ice balls were disregarded.

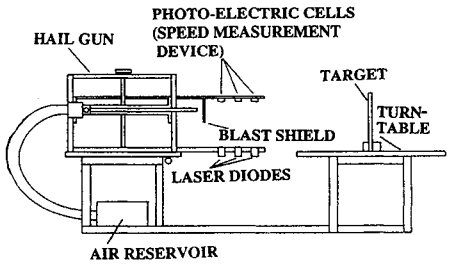

Fig. 1 Experimental arrangement.

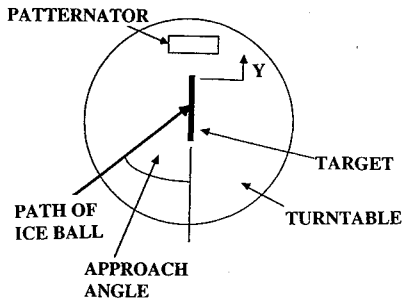

Fig. 2 Plan view of flat plate and turntable arrangement.

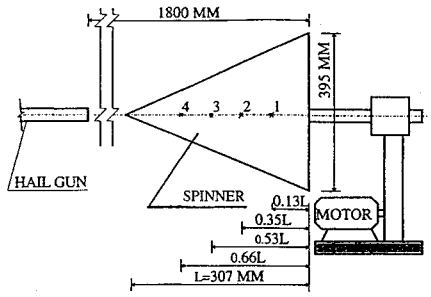

Fig. 3 Arrangement for tests on spinner.

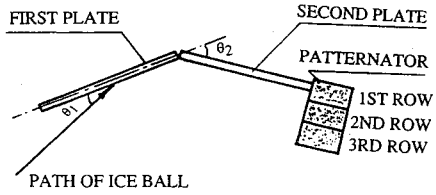

Fig. 4 Arrangement for secondary impact studies.

The steel flat plate is shown as the target in Figs. 1 and 2. This measured 350 by 200 mm and was 5 mm thick. The turntable was used to vary the approach angle of the ice ball relative to the flat plate. For all of the flat-plate results reported here the patternator was placed at $Y = 0$ mm (i.e., the patternator elements immediately behind the edge of the plate). The hail gun was targeted at a point midway along the short side of the plate and 100 mm down from the top edge. For the spinner tests, the flat plate was replaced by a spinner from a Rolls–Royce Tay engine. The patternator was positioned immediately behind the base of the spinner. The hail gun was targeted at the four different axial positions shown in Fig. 3. Depending on the target position, the ice balls either hit a composite fiber or steel surface. Rotation of the spinner was achieved by using a small dc electric motor. The arrangement of the targets for the secondary impact studies is shown in Fig. 4. The ice ball approached at an angle of θ_1 and impacted upon the first flat plate. The second flat plate was placed adjacent to the first plate at an angle θ_2, with the patternator placed immediately behind the edge furthest away from the first plate. The gap between the first and second plates was sealed for all tests.

The ice fragments and water resulting from the impact were collected in a patternator that consisted of elements manufactured from 25.5-mm-square steel tube (wall thickness 0.8 mm). After the run consisting of at least 25 ice balls, the contents of each element were weighed using a balance with a nominal accuracy of 0.02 g. The amount of ice caught in a single element ranged between 0–10 g. For the spinner tests, it was not possible to arrange the square patternator elements to accurately follow the circumference of the spinner base. Therefore, a mask was placed over the patternator to provide a 10-mm-wide slot, whose lower edge followed the spinner base.

As an alternative to the patternator, the impact was recorded using high-speed photography. For the flat plate, the front lighting technique was used. To provide information on the third dimension (i.e., looking down on the horizontal plane of the impact) a plane mirror was placed 45 deg above the plate. The camera was positioned normal to the plate and arranged so that the image in the mirror formed the top half of the field of view and the real ice ball and impact formed the lower half. The mirror was formed by silvering the top surface of a piece of glass. Consequently, the image of the impact was reflected on the top surface of the mirror, so that no account had to be taken of the depth of the image behind the mirror when analyzing the film.

For most of the runs a conventional high-speed cine camera was used at a speed of 6000 frames/s. Analysis of the film was carried out using a system originally developed for particle image velocimetry laser experiments, to give velocity and direction of travel. Some of the high-speed photography runs were carried out using an image converter camera. This type of camera uses a single negative rather than cine film. For the present study, the advantage of the camera lay with its high frame speed (up to 20 million frames/s) achieved because the scanning is carried out electronically rather than mechanically as in the cine camera. Typically, 40,000 frames/s were used.

A similar experimental arrangement was used for the spinner, although it proved impractical to use the mirror. To obtain data on all three dimensions of the impact, it was necessary to carry out separate runs with the camera in two different positions (i.e., one camera position viewing the spinner from the side, the other viewing the spinner from the top). For the secondary impact studies, the camera was placed normal to the second plate. The mirror was positioned at 45 deg above the second plate to provide information on the third dimension of the secondary impact.

Parameters Investigated

The flat plate results presented consider the influence of the following:

1) The approach velocity of the ice ball relative to the target: this corresponds to different descent speeds for an aircraft.

2) The approach angle of the ice ball relative to the target: this is important because due to geometric twist along a fan blade, fan blade section profile, rotational speed of the fan, etc., a hailstone will approach the surface of a fan blade with a range of possible approach angles.

3) Target temperature: all of the experiments were carried out in ambient atmospheric conditions at ground level. Hail can be encountered at heights up to 6000 m where the static temperature of the atmosphere is below freezing. The fan stage components under the most severe hail storm conditions are likely to be at a temperature around 0°C. Therefore, at altitude, the temperature of the fan will be significantly less than the ambient temperature in a ground-level laboratory.

For the spinner, the influence of rotation and ice ball approach velocity are considered. In addition the similarities and differences between the spinner and flat plate results will be highlighted. For the secondary impact studies the angle of the second plate θ_2 was varied, with the approach angle θ_1 and the approach velocity of the ice ball remaining fixed.

It is not suggested that the influences mentioned previously are the only important parameters affecting the impact characteristics of hailstones. Investigations into the importance of other possibly relevant parameters are continuing.

Flat Plate with Approach Angle = 45 Deg and Mach Number = 0.5

This arrangement with the patternator at $Y = 0$ represented a standard reference condition for the patternator tests. It was repeated on a number of occasions to ensure that no unexplained or unexpected influences, which varied with time, were affecting the experimental setup. As the results remained repeatable throughout the test program, there is a high degree of confidence that any change in patternator results can be attributed to the parameter being varied. The results for a number of different runs are shown in Fig. 5. The vertical axis is the normalized ice caught, i.e., the ice and water caught by an individual element, divided by the total ice and water caught by the patternator. The horizontal axis represents the height of the center of the patternator element above, or below, the impact point on the plate. For the purposes of plotting the results, all of the ice and water caught by an element has been plotted at the height, corresponding to the center of the element. For the run-to-run repeatability, it can be seen that at the worst the spread in the data for any given element is less than 3%. This is reasonable repeatability given that no two ice balls are likely to break up in exactly the same way, and as a result some scatter in the distribution curves would be expected.

The results shown in Fig. 5 are for the single vertical row of patternator elements immediately behind the edge of the plate. The results for the other vertical rows, typically accounted for less than 0.5% of the total ice caught. This implies that the ice fragments and water resulting from an impact moved almost along the surface of the plate. To calculate the angle at which the impact debris (ice fragments and water) left the plate's surface, the patternator was moved away from the plate to a position $Y = 225$ mm. Further runs were carried out, which showed that typically over 97% of the debris was caught by a single row of patternator elements. From simple geometry it can be shown that this 97% of impact debris left the plate with bounce angle of less than 2.25 deg. This low bounce angle was confirmed by high-speed photography. Figure 6 shows a series of photographs taken by the image converter camera. The upper image in each photograph is the mirror view, i.e., looking down on the impact, and from this view it can be seen that there is very little motion normal to the plate. The low bounce angle was typical for all of the single impact cases presented in this article.

A significant feature of the distributions in Fig. 5 is the sharpness of the peaks, implying that most of the debris resulting from an impact was concentrated in a narrow wedge (or cone) leaving the impact point. To illustrate this, the patternator distributions can be plotted as shown in Fig. 7. The spread angle is the angle subtended by a line along the surface of the plate joining the impact point to the center of a patternator element. For convenience the horizontal axis has been plotted as a semispread angle. A semispread angle of, e.g., 15 deg, corresponds to a spread angle of 30 deg (i.e., between +15 and −15 deg). The vertical axis has been determined by summing the debris caught by all of the patternator elements within a given spread angle. This sum then has to be plotted as a fraction of the total ice caught by the patternator. For an approach angle of 45 deg, it can be seen that 90% of the debris is contained with a wedge of 30-deg semi-included angle (i.e., semispread angle). The idea of the wedge is reinforced by the high-speed photography (Fig. 6). The lower image in each photograph shows the impact on the front face of the plate. The ice ball can be seen to impact on the plate with the debris fanning out in a wedge from the impact point. The semi-included angle of the wedge appears larger in the high-speed photographs than the 30 deg determined from the patternator. This is because the wedge containing all of the ice is viewed in the photographs.

The high-speed photographs allowed the behavior of the debris resulting from the impact to be studied. Immediately after impact a cloud of particles was formed that moved rap-

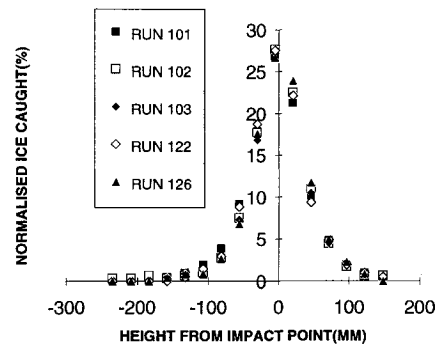

Fig. 5 Repeatability of normalized ice caught distributions for flat plate.

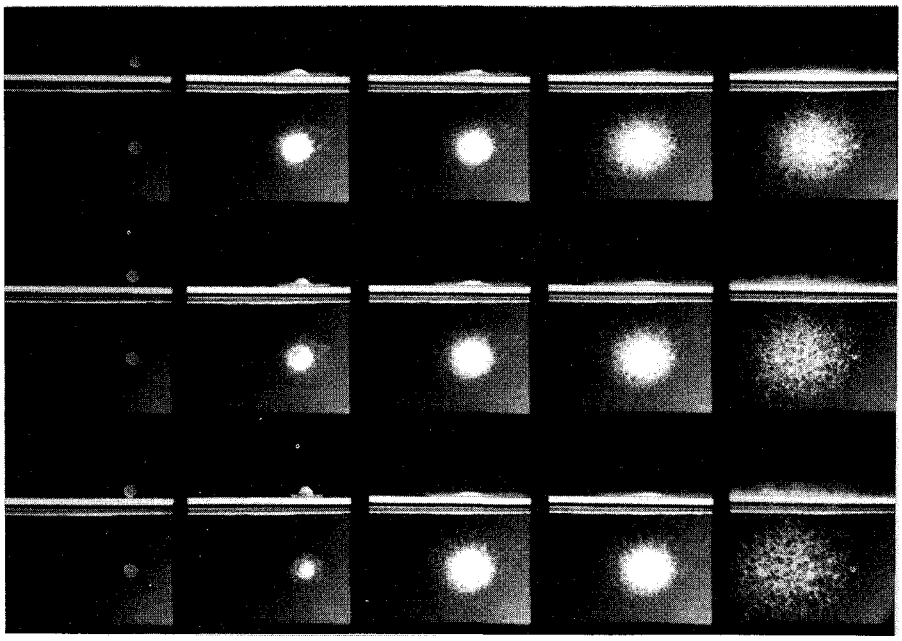

Fig. 6 Photograph of ice ball impact; flat plate; approach angle = 45 deg; Mach number = 0.5.

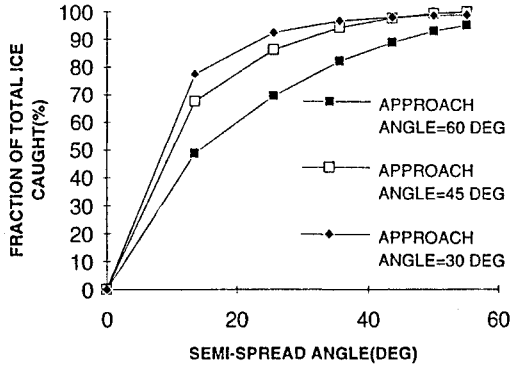

Fig. 7 Ice caught vs semispread angle; flat plate; Mach number = 0.5.

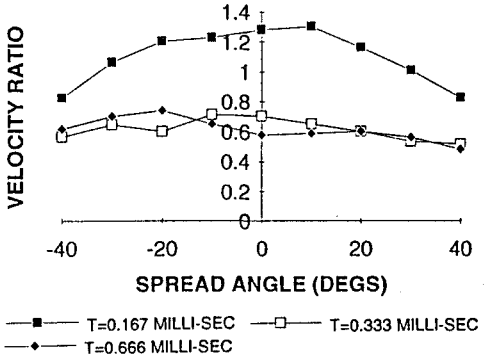

Fig. 8 Velocity ratio for cloud of particles.

idly along the plate. The initial velocity of the fastest moving particles (i.e., the leading edge of the cloud) was greater than the approach velocity of the ice ball, suggesting a significant release of kinetic energy during the impact. As the cloud moved away from the impact point the velocity of the particles decreased fairly rapidly. The behavior of this cloud is illustrated by Fig. 8. This figure is for one ice ball and the results have been obtained by analysis of high-speed cine film. The vertical axis is the velocity ratio, i.e., the velocity of the leading edge of the cloud divided by the approach velocity of the ice ball. The spread angle is the angle above or below the centerline of the cloud, at which the velocity ratio was determined. The curves show the velocity ratios at time T after the impact. The time $T = 0$ is taken as the end of the frame of cine film showing the hailstone impacting on the surface. The impact occurred while this frame was exposed, but it was impossible to tell at what time during the frame's exposure the impact actually occurred. Therefore, there is some error in the quoted values of T. The maximum error is 0.167 ms, which is the exposure time of the frame. The photographs from the image converter camera confirmed that initial velocities after impact were significantly greater than the approach velocity of the ice ball. In fact, the photographs showed that the velocities of the fine particles given off in the first 25 μs of the impact were typically greater than 450 m/s (velocity ratio = 2.6). These particles decelerated rapidly, and 75 μs after impact their absolute velocities were typically halved. The resolution and frame speed of the high-speed cine camera was too low to pick up the finest particles. However, the fine particles represented a small fraction of the mass of the impacting ice ball.

Both high-speed photography techniques were unable to define the size or velocities of individual ice particles in the cloud. However, at the end of the impact it was possible to measure the velocities of the last particles. These velocities were typically around 20 m/s (velocity ratio = 0.11). Inspecting frames 13, 14, and 15 of Fig. 6, it is interesting to note that the last particles to leave the impact point included both large and small particles. In fact, the large particles appear to be distributed throughout the cloud, suggesting that they don't all originate from the same part of the ice ball.

From the mirror views of Fig. 6 it is possible to determine at what stage after impact the ice ball ceases to be identifiable and can be assumed to be completely broken up. This occurs at around frame 9 (i.e., 175 μs after impact). This elapsed time (or crushing time) indicates that the velocity of the ice ball normal to the plate reduced during the impact. If this

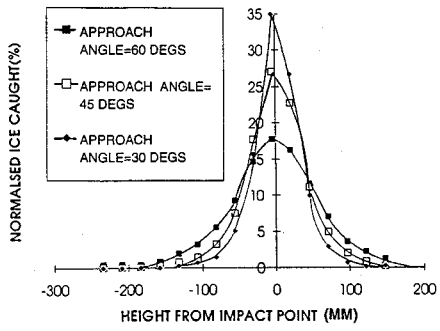

Fig. 9 Distribution of normalized ice caught for three approach angles; flat plate; Mach number = 0.5.

wasn't the case, the crushing time given by dividing the ice ball's diameter by its approach velocity normal to the plate would be approximately 100 μs. Clearly from Fig. 6 (frame 7), the ice ball is still identifiable 100 μs after impact and has not completely broken up.

Influence of Approach Angle

The influence of approach angle on the distributions of normalized ice caught is shown in Fig. 9. Increasing the approach angle served to make a more uniform distribution of ice and water across the patternator, i.e., the peak value at the impact height was reduced and values displaced some distance from the impact height increased. Looking at the same results in terms of total ice caught against a semispread angle (Fig. 7) suggests that the debris left the impact point within a wedge whose spread angle increased with increasing approach angle. Intuitively, from considering the extreme approach angles of 90 and 0 deg this trend appears to be correct. At 90 deg, the ice ball is approaching normal to the plate. Debris from the impact would be expected to be evenly distributed in a circle about the impact point, i.e., a "large" spread angle. At the other extreme of 0 deg, the ice ball would pass tangentially along the surface of plate and straight into one patternator element, without breaking up, i.e., a spread angle of 0 deg.

As with the 45-deg plate angle, virtually all of the debris (typically 97%) was caught in the vertical row of patternator elements immediately behind the edge of the plate. Again, it was concluded that the debris left the impact point at a shallow bounce angle relative to the surface of the plate. The size of the patternator elements was relatively coarse, and no attempt was made to determine whether the bounce angle changed with approach angle. High-speed cine photography verified that the ice ball impact was characterized by a low bounce angle for all approach angles. Cine film also verified that the semi-included angle of the wedge decreased as the approach angle decreased, and that for all approach angles the impact was characterized by a cloud of particles leaving the impact point at high speed, but slowing down as they moved along the plate.

Influence of Approach Velocity

The approach velocity of the ice ball was varied between 100–175 m/s (Mach numbers of 0.3–0.5). The main conclusion was that approach velocity had little influence on the distribution of debris following impact. The results still displayed symmetry about the impact height, and as for all the cases already discussed, typically 97% of the debris was caught in a single vertical row of patternator elements implying that the debris left the plate at a low bounce angle. This lack of change with Mach number was verified by high-speed cine photography. The impacts at a Mach number of 0.3 were similar to those observed for a Mach number of 0.5, i.e., low bounce angle and a cloud of particles initially moving rapidly away from the impact point.

Influence of Plate Temperature

To investigate the influence of plate temperature the plate was cooled in a freezer to −14°C. The plate was then installed on the turntable. During this installation and the subsequent testing, the plate was warmed by the surrounding ambient conditions. To reduce the rate of increase in temperature an ice pack was placed against the nonimpact surface of the plate. During the tests the temperature of the plate was monitored by a thermocouple. Each test was terminated when the plate temperature had increased by 5°C from its value when the first ice ball was fired. The mean plate temperature during the tests was around 0°C. At this temperature no significant difference in the distributions when compared with Fig. 5 could be determined. This indicated that work on hail impact characteristics can be carried out at ambient temperatures significantly higher than freezing. High-speed photography tests were not conducted for the cooled plate, because it was impractical to keep the plate temperature close to 0°C in the presence of the photographic lighting.

Stationary Spinner

Typical patternator results for the stationary spinner are shown in Fig. 10. These results are for three separate runs with the ice balls impacting at point 2 on the spinner surface (Fig. 3). For convenience the data in Fig. 10 have been plotted in a different format from the flat plate results. The horizontal axis is the angular position of the center of each patternator element measured at the circumference of the base of the spinner. The vertical axis is given by normalized ice caught divided by the length of the patternator element in degrees of arc of the circumference of the spinner base. The distributions shown in Fig. 10 indicate that the patternator produced a reasonable degree of repeatability. Increasing the slot width to 15 mm did not change the shape or level of the distribution. Nor did it increase the total amount of ice caught by the patternator. This indicated that all the debris from the impact lay close to the spinner surface and that there was a low bounce angle. For the shot point being considered, the 10-mm-wide slot indicated a bounce angle of less than 4.5 deg. The low bounce angle was confirmed by high-speed cine.

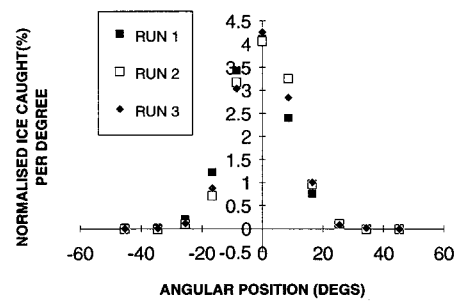

Fig. 10 Repeatability of distributions; stationary spinner; shot point 2; Mach number = 0.5.

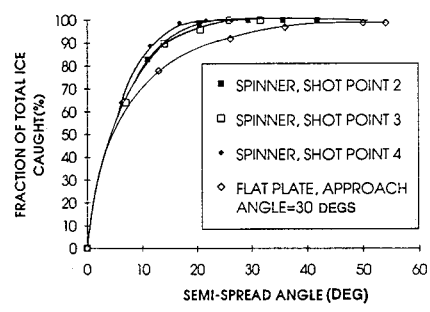

Fig. 11 Ice caught vs semispread angle for stationary spinner and flat plate; Mach number = 0.5.

As with the flat plate results, the distribution was symmetrical about the central patternator element (i.e., symmetrical about the impact point). The shape of the curve was dependent on the point of ice ball impact on the spinner. Moving the impact point towards the apex of the spinner (shot points 3 and 4) depressed the peak values and increased the amount of ice caught away from the center. This "flattening out" of the distribution as the impact point moved away from the patternator (i.e., towards the tip) reinforces the concept of a wedge of debris spreading out from the impact point. The idea of the wedge is more clearly seen by plotting in terms of semispread angles (Fig. 11). It can be seen that the data from all shot points collapse about a single curve. Also shown in Fig. 11 are the data for the flat plate with an approach angle of 30 deg. This roughly corresponds to the approach angle for the spinner (i.e., half the spinner apex angle, 28.5 deg). It is pleasing that around a semi-included angle of 35 deg the spinner and flat-plate results agree. The differences between flat plate and spinner at lower spread angles are probably due to the relative coarseness of the patternator elements for the flat plate. In moving from shot point 2 to 3 the impact surface changed from steel to composite. As can be seen from Fig. 11 there was no discernable change in the distribution of debris resulting from the impact.

High-speed cine photography showed that upon impact the ice ball broke up into a cloud of particles that moved away rapidly. Comparing the velocity ratios of the cloud for the spinner with those for the flat plate showed no significant differences.

Influence of Spinner Rotation

The spinner was rotated at two speeds, 1900 and 2300 rpm. The upper speed was limited by the power available from the small electric motor used to rotate the spinner. Figure 12 shows that rotation produced no significant change in the distribution of debris when compared with the stationary spinner case. The spread in the data lies within the repeatability bands previously discussed for the stationary spinner. In fact, repeatability tests were carried out on the rotating spinner and these produced results similar to those for the stationary spinner. As with the flat plate, there was no measurable change in the distribution of debris for the rotating spinner with a change in approach velocity of the ice ball. Tests were carried out at approach velocities down to 100 m/s (Mach number = 0.3). High-speed cine photography showed that the initial velocity ratio of the cloud of debris for the rotating spinner was similar to those observed for the flat plate.

Secondary Impact Studies

All of the secondary impact studies were carried out at an approach angle θ_1 of 30 deg and approach Mach number of 0.5. The patternator results for a second plate angle θ_2 of 15 deg are shown in Fig. 13. Like the flat-plate results shown in Fig. 5, most of the debris was concentrated in the single vertical row of patternator elements immediately behind the edge of the second plate (row 1). As the second plate angle was increased the proportion of ice caught by the second vertical row of elements (row 2) increased, and eventually significant amounts of ice were also caught by the third row of elements (row 3). This is illustrated by Fig. 14. The first row of patternator elements corresponded to a bounce angle up to 3.5 deg, the second row between 3.5–10 deg, and the third row between 10–16.5 deg. These results suggest that high debris bounce angles can be achieved from secondary impacts, whereas for a single flat plate the bounce angle was typically around 2.25 deg. High-speed cine photography confirmed the high bounce angles for secondary impacts and revealed some information on the nature of the impacts. Following impact on the first plate, a cloud of particles moved rapidly away and decelerated before impacting on the second plate and breaking up into smaller particles. The high bounce angle was seen to be brought about by particles moving from the first plate colliding with debris from particles that had already impacted on the second plate.

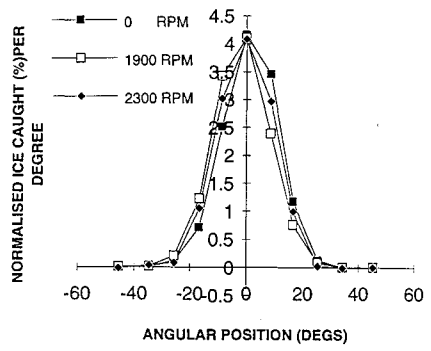

Fig. 12 Influence of spinner rotation on distribution of ice; Mach number = 0.5.

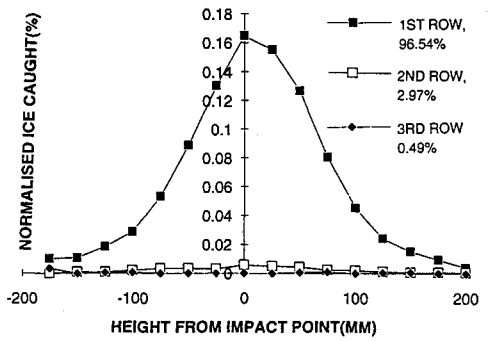

Fig. 13 Distribution of normalized ice caught for secondary impact; Mach number = 0.5; θ_1 = 30 deg and θ_2 = 15 deg.

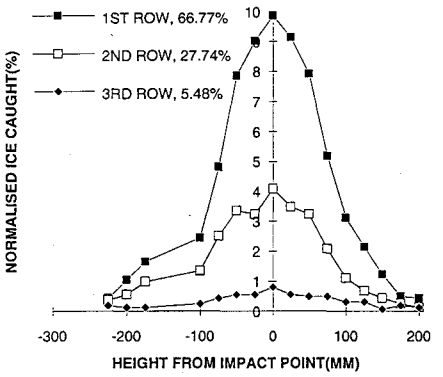

Fig. 14 Distribution of normalized ice caught for secondary impact; Mach number = 0.5; θ_1 = 30 deg and θ_2 = 45 deg.

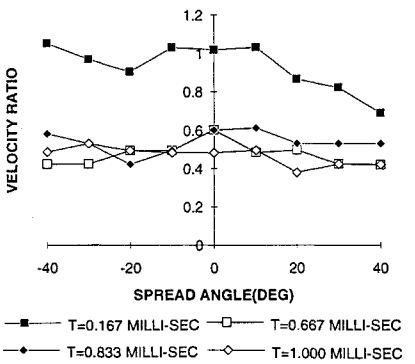

Fig. 15 Velocity ratio for cloud of particles. Secondary impact; Mach number = 0.5; θ_1 = 30 deg and θ_2 = 45 deg.

High-speed photography was also used to determine the velocity ratios of the fastest moving particles at the leading edge of the cloud (Fig. 15). The times quoted in Fig. 15 are after the impact on the first plate, and are subject to the same errors previously discussed for Fig. 8. The curve labeled T = 0.667 ms is the first velocity ratio after impact on the second plate. The curves for T = 0.333 and 0.501 ms have been removed for clarity; however, the levels were similar to those of Fig. 8. Referring to Fig. 15 it can be seen that the velocity ratios following secondary impact were lower than for the first impact. This is to be expected because the velocities of the particles immediately prior to the second impact were significantly less than the approach velocity of the original ice ball. Unlike the single impacts on a plate, there was no rapid deceleration of the particles from the secondary impact.

Conclusions

For the impact of an ice ball on a flat plate or spinner the following conclusions can be made:

1) Ice ball impacts are characterized by low bounce normal to the surface, with the debris leaving the impact point in a wedge. The semi-included angle of this wedge is a function of the approach angle of the ice ball.

2) The initial velocities of the fastest moving particles in the wedge are significantly higher than the approach velocity of the ice ball. However, these particles decelerate rapidly.

3) The time taken for the ice ball to disintegrate (i.e., the crushing time) is relatively long.

4) For secondary impacts the bounce angle of the debris is a function of the angle between the first and second surfaces.

Acknowledgments

The program has been funded by Rolls–Royce, plc. and the Science and Engineering Research Council. Additional funding has been provided by the Civil Aviation Authority. The photographs of the ice ball impact were obtained with the help of NAC Europe.

References

[1]Define, K., "Inclement Weather Induced Aircraft Engine Power Loss," AIAA Paper 90-2169, July 1990.

[2]Murthy, S. N. B., "Transient Performance of Fan Engine with Water Ingestion," AIAA Paper 91-1897, June 1991.

[3]Render, P. M., Pan, H., Sherwood, M., and Riley, S. J., "Studies into the Hail Ingestion Characteristics of Turbofan Engines," AIAA Paper 93-2174, June 1993.